

Magnetically Actuated PVA-Gelatin-Fe₃O₄ Based Magnetic Hydrogel Microrobot

Abhijeet Tanaji Patil, Pranav Shivshankar Shirolkar, Pranav Prashant Bahulekar, Aditya Sandip Kadam,
Prathamesh Rajaram Patil, Siddhesh Eknath Gawade, Dr. K. T. Jadhav, Chinmay Pisal

Department Of Chemical Engineering
D.Y. Patil College Of Engineering & Technology Kolhapur-416006

Abstract - The advancement of bioengineered microrobots has opened new possibilities in biomedical engineering, particularly for minimally invasive therapeutic applications. In this study, a polyvinyl alcohol (PVA)-gelatin-Fe₃O₄ based magnetic hydrogel microrobot is developed for magnetically actuated hyperthermia. The microrobot is fabricated using biocompatible polymers, PVA and gelatin, which provide a flexible and stable hydrogel network, while superparamagnetic Fe₃O₄ nanoparticles are incorporated to impart magnetic responsiveness. Physicochemical and rheological analyses confirm the formation of a stable, elastic, and biocompatible system suitable for physiological environments. Upon exposure to an external alternating magnetic field (AMF), the embedded Fe₃O₄ nanoparticles enable wireless magnetic actuation, facilitating controlled locomotion and precise navigation. Simultaneously, magnetic induction generates localized heat, achieving therapeutic temperatures in the range of 42–45 °C required for effective cancer cell ablation. This dual functionality enables both targeted movement and localized hyperthermia, minimizing damage to surrounding healthy tissues. Additionally, the hydrogel matrix offers potential for drug loading and controlled release, further enhancing its applicability in targeted therapy.

Keywords: PVA-Gelatin Hydrogel, Magnetic Microrobot, Fe₃O₄ Nanoparticles, Magnetic Actuation.

INTRODUCTION

The field of biomedical engineering has witnessed rapid advancements with the emergence of microrobotic systems designed to operate at micro- and nanoscale dimensions within complex biological environments. These microrobots have opened new possibilities for minimally invasive diagnosis and therapy by enabling precise intervention at targeted sites inside the human body. Conventional treatment strategies, particularly in cancer therapy, often suffer from limitations such as poor targeting efficiency, systemic toxicity, and lack of controlled delivery. In this context, microrobots offer a transformative approach by combining controlled navigation, site-specific action, and multifunctionality, thereby enhancing therapeutic efficacy while minimizing side effects (1). Among the various classes of microrobots, soft hydrogel-based systems have gained considerable attention due to their intrinsic biocompatibility, flexibility, and structural similarity to natural tissues. Hydrogels are three-dimensional polymeric networks capable of retaining large amounts of water, which makes them highly suitable for biomedical applications. Polymers such as polyvinyl alcohol (PVA) and gelatin are widely used in hydrogel fabrication owing to their non-toxic nature, biodegradability, and excellent mechanical properties. PVA contributes to mechanical strength and stability, while gelatin enhances biological interactions and cellular compatibility. The combination of these polymers results in a hybrid hydrogel system that exhibits both robustness and biofunctionality, making it an ideal candidate for microrobotic applications (2).

To impart active functionality and external controllability, the incorporation of magnetic nanoparticles into hydrogel matrices has emerged as a powerful strategy. Superparamagnetic iron oxide (Fe₃O₄) nanoparticles are particularly attractive due to their strong magnetic responsiveness, chemical stability, and proven biocompatibility. When embedded within a hydrogel network, these nanoparticles enable remote actuation of microrobots using external magnetic fields. Magnetic actuation offers several advantages, including wireless control, deep tissue penetration, high spatial precision, and real-time manipulation without the need for onboard power sources (3). This capability is crucial for navigating microrobots through complex biological fluids and reaching otherwise inaccessible regions within the body. In addition to enabling locomotion, Fe₃O₄ nanoparticles exhibit the ability to generate heat when subjected to an alternating magnetic field (AMF) through mechanisms such as Néel and Brownian relaxation losses. This phenomenon forms the basis of magnetic hyperthermia, a promising therapeutic technique for cancer treatment. By raising

the local temperature to a therapeutic range of 42–45 °C, cancer cells can be selectively destroyed due to their higher sensitivity to heat compared to normal cells. The integration of magnetic hyperthermia with microrobotic systems allows simultaneous targeting and treatment, thereby overcoming the limitations of conventional hyperthermia approaches, which often lack spatial precision (4).

The concept of magnetically actuated hydrogel microrobots represents a convergence of soft robotics, nanotechnology, and biomedical engineering. These systems combine the advantages of hydrogel materials—such as deformability, biocompatibility, and drug-loading capability—with the remote controllability of magnetic nanoparticles. Such microrobots can be engineered to perform multiple functions, including targeted drug delivery, localized heating, and controlled release of therapeutic agents. Furthermore, their soft nature minimizes mechanical damage to surrounding tissues, making them particularly suitable for in vivo applications. Despite these promising attributes, several challenges remain in the development of efficient hydrogel microrobots, including achieving optimal mechanical strength, ensuring uniform distribution of magnetic nanoparticles, and maintaining stable actuation under physiological conditions. Additionally, the design of microrobots that can simultaneously achieve controlled locomotion and effective hyperthermia requires careful optimization of material composition and structural properties (5).

The present study focuses on the development of a polyvinyl alcohol (PVA)–gelatin–Fe₃O₄ based magnetic hydrogel microrobot with enhanced actuation and therapeutic capabilities. The proposed system aims to integrate biocompatible polymer networks with superparamagnetic nanoparticles to achieve dual functionality—precise magnetic navigation and efficient localized hyperthermia. Through systematic fabrication and characterization, this work explores the physicochemical, rheological, and magnetic properties of the microrobot, along with its response under an external alternating magnetic field (6). Magnetic hydrogel microrobots represent an advanced class of smart materials that integrate biocompatible polymer networks with magnetic nanoparticles to achieve multifunctional performance. These systems are typically fabricated using polymers such as polyvinyl alcohol (PVA) and gelatin, which provide flexibility, biodegradability, and tissue-like properties. The incorporation of Fe₃O₄ nanoparticles into the hydrogel matrix imparts magnetic responsiveness, enabling external control without direct contact. The resulting structure forms a soft, stable, and porous three-dimensional network in which magnetic nanoparticles are uniformly distributed, allowing the material to respond efficiently to applied magnetic fields (7).

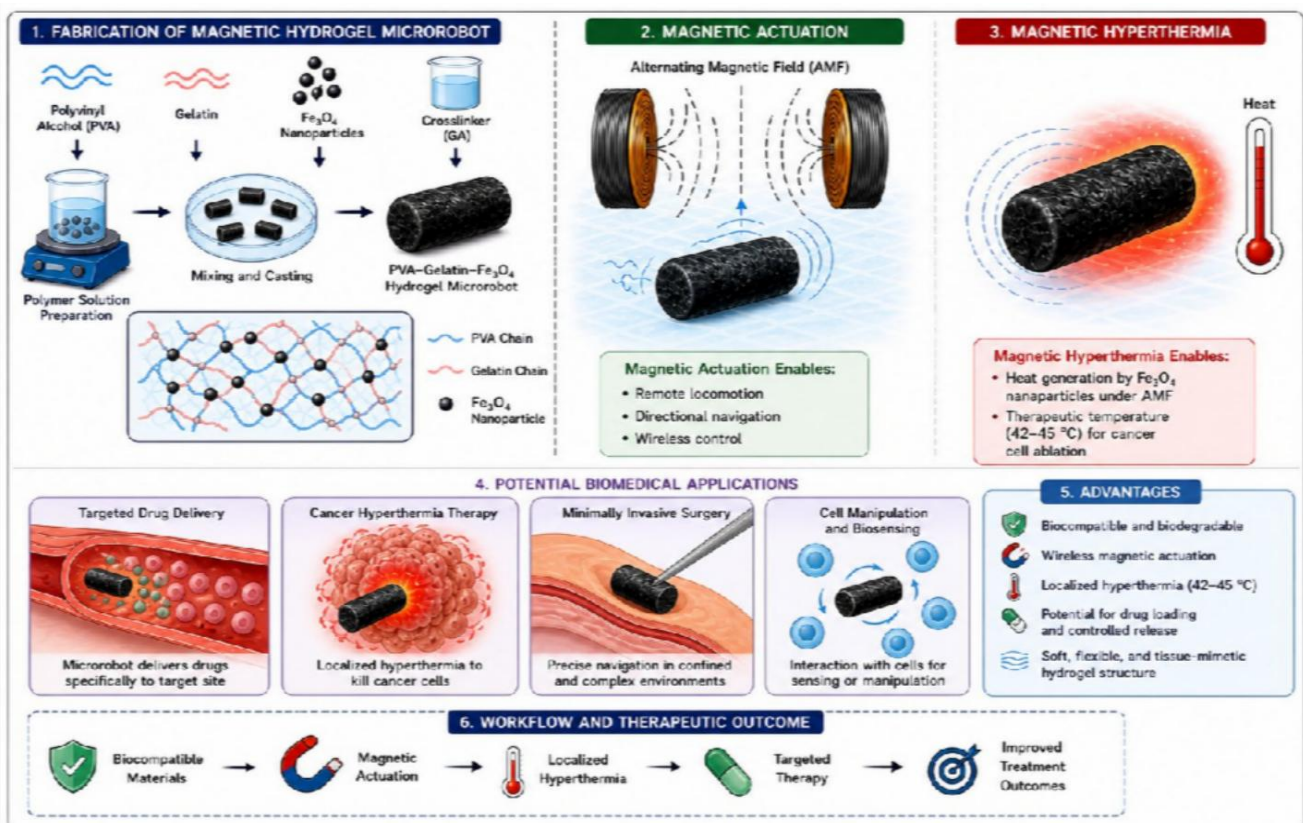


Figure No. 1.1: Schematic Representation of Magnetic Hydrogel Microrobot: Fabrication, Actuation, Hyperthermia, and Biomedical Applications

Under an external magnetic field, these microrobots exhibit controlled motion, including translation, rotation, and directional navigation, making them suitable for remote actuation in fluidic and biological environments. Additionally, when exposed to an alternating magnetic field, the embedded magnetic nanoparticles generate localized heat due to magnetic relaxation losses, enabling applications such as magnetic hyperthermia. The combination of controlled movement and heat generation allows these systems to perform targeted therapeutic functions, including site-specific drug delivery and localized cancer treatment. Overall, magnetic hydrogel microrobots offer significant advantages such as wireless control, minimal invasiveness, biocompatibility, and multifunctionality, making them highly promising for future biomedical and clinical applications (8).

LITERATURE SURVEY

Table No 2.1: Literature review of Related Work

Sr.No	Material	Nano Particles	Characterization	Application	Reference
1	Polydopamine, PVA,PAA	Fe ₃ O ₄	SEM, TEM, FTIR	Tissue Engineering	(9)
2	Polyvinyl alcohol, Gelatin	-	FTIR	Drug Delivery	(10)
3	Chitosan	Fe ₃ O ₄	FTIR	Soft and wearable electronics	(11)
4	Alginate and methyl cellulose	-	FTIR	3D , 4D Printing	(12)
5	Polyvinyl alcohol + nanofibrillated cellulose	M _n Fe ₂ O ₄	FTIR, SEM	Electrochemical display deliver , rechargeable battery	(13)
6	Polyacrylamide acrylamide	Fe ₃ O ₄	SEM	Magnetic hyperthermia, Tissue Engineering	(14)
7	Alginate + polyacrylamide	Fe ₃ O ₄	SEM, TEM	Cantilever bending beam	(15)
8	Poly(N-isopropylacrylamide)	-	AMF	SoftRobotics, biomedical engineering	(16)

Magnetic hydrogel microrobots represent an emerging class of smart, multifunctional materials that integrate the soft, hydrated nature of hydrogels with the remote controllability of magnetic nanoparticles. Various polymers such as polyvinyl alcohol (PVA), chitosan, alginate, polyacrylamide, and poly(N-isopropylacrylamide) have been widely explored due to their biocompatibility, flexibility, and tunable physicochemical properties. Incorporation of magnetic nanoparticles like Fe₃O₄ and MnFe₂O₄ enables external magnetic field responsiveness, which is a key feature for microrobotic applications. Hybrid systems such as PVA–PAA and alginate–polyacrylamide networks exhibit enhanced mechanical stability due to interpenetrating polymer networks (IPNs), which are particularly useful in applications requiring structural integrity under deformation, such as cantilever-based systems and soft actuators. Similarly, natural polymers like gelatin and chitosan contribute to improved biocompatibility and biodegradability, making them highly suitable for biomedical applications including drug delivery and tissue scaffolding. The absence or presence of magnetic nanoparticles directly influences the functionality, where non-magnetic hydrogels are more suitable for passive roles like 3D/4D printing, while magnetic nanocomposites enable active control. The incorporation of magnetic nanoparticles such as Fe₃O₄ and MnFe₂O₄ significantly enhances the functional capabilities of hydrogels by imparting magnetic responsiveness, enabling remote actuation and controlled movement under external magnetic fields. These properties are particularly important in the development of magnetic hydrogel microrobots, where precise navigation and targeted action are

required. Studies involving polyacrylamide-based magnetic hydrogels demonstrate their effectiveness in magnetic hyperthermia and tissue engineering, indicating their dual functionality in therapy and structural support. Moreover, the use of advanced characterization techniques like SEM and TEM provides insight into nanoparticle dispersion and pore structure, which directly affect diffusion-controlled processes such as drug release and actuation efficiency.

Furthermore, emerging applications such as soft robotics and biomedical microrobotics are increasingly leveraging stimuli-responsive hydrogels like poly(N-isopropylacrylamide) (PNIPAM), which exhibit temperature and magnetic field sensitivity. These smart materials enable reversible shape transformation and controlled deformation under alternating magnetic fields (AMF), making them ideal candidates for designing soft microrobotic systems capable of complex movements. The integration of such materials into microrobotic platforms opens new avenues for minimally invasive procedures, including targeted drug delivery, localized therapy, and micro-manipulation in biological environments. Overall, the literature emphasizes that the synergistic combination of polymer chemistry, magnetic nanoparticles, and external field control is key to advancing the performance and applicability of magnetic hydrogel microrobots. A comprehensive literature survey is essential to understand the progress made in the design, synthesis, characterization, and application of various magnetic hydrogel systems. The following studies highlight different polymer compositions, types of magnetic nanoparticles, characterization techniques, and application areas, providing a strong foundation for the development of advanced magnetic hydrogel microrobots with improved performance and multifunctionality.

Furthermore, the table provides insights into the characterization techniques employed to evaluate these systems, including SEM, TEM, FTIR, and XRD. These techniques confirm the structural integrity, chemical interactions, crystallinity, and morphology of the developed hydrogels. For instance, SEM and TEM analyses reveal pore structure and nanoparticle distribution, which are crucial for drug loading and release behavior, while FTIR and XRD confirm successful incorporation of components and phase purity. In addition, the table emphasizes the role of magnetic nanoparticles in defining the actuation and functional behavior of the hydrogel systems. Nanoparticles such as Fe_3O_4 and MnFe_2O_4 are most commonly used due to their strong magnetic properties and biocompatibility. Their concentration, size, and distribution within the hydrogel matrix directly influence key properties such as magnetic responsiveness, heating efficiency, and motion control. This is particularly important for applications like magnetic hyperthermia and targeted drug delivery, where precise control over movement and heat generation is required. The application-focused studies summarized in the table demonstrate the versatility of magnetic hydrogels in areas such as soft robotics, biosensing, tissue engineering, and minimally invasive therapy. The comparative analysis presented in the table reinforces the importance of material selection, structural design, and synthesis strategy in determining the performance of magnetic hydrogel microrobots. It clearly shows that the integration of suitable polymer networks with optimally dispersed magnetic nanoparticles leads to enhanced multifunctionality. This systematic understanding of previously reported studies provides a strong foundation for designing next-generation magnetic hydrogel microrobots with improved efficiency, controllability, and application-specific performance.

OBJECTIVES

1. To design and fabricate a PVA- Gelatin- Fe_3O_4 based magnetic hydrogel microrobot.
2. To evaluate its physio-chemical and rheological characterizations.
3. To study the magnetic actuation behavior of the hydrogel microrobot under an alternating magnetic field.

METHODOLOGY

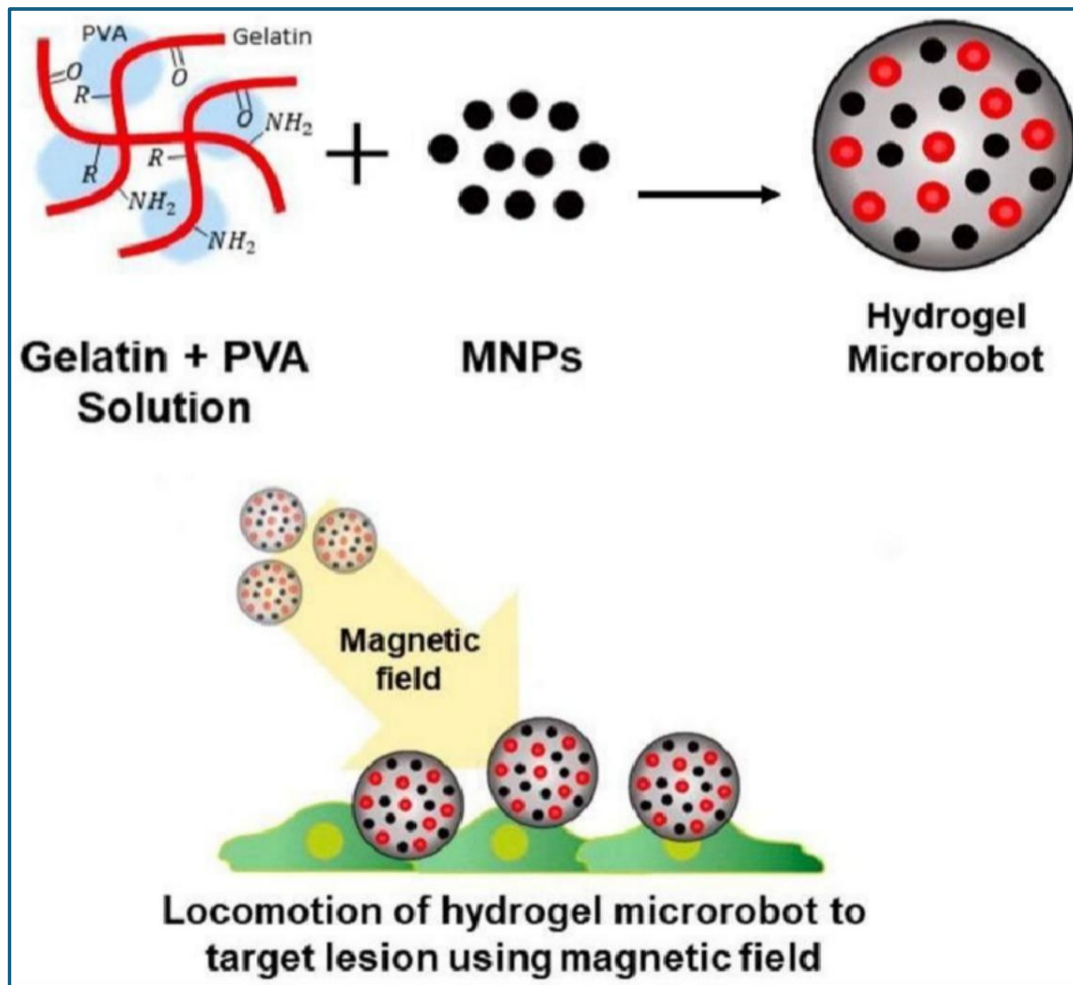


Figure No. 4.1: Synthesis of magnetic hydrogel microrobot and Locomotion of hydrogel micro-robot to target lesions.

MATERIALS REQUIRED:

1. PVA(Polyvinyl alcohol)
2. Gelatin
3. $\text{FeCl}_2 \cdot 4\text{H}_2\text{O}$ and $\text{FeCl}_3 \cdot 6\text{H}_2\text{O}$ (for Fe_3O_4 synthesis)
4. Ammonia
5. Crosslinking agents
6. Buffer solutions (PBS/acetate buffer)

4.1 SYNTHESIS OF Fe_3O_4 NANOPARTICLES (CO-PRECIPIATION METHOD)

Fe_3O_4 nanoparticles are synthesized using the co-precipitation technique, which is widely preferred due to its simplicity, scalability, and cost-effectiveness. In this method, ferrous (Fe^{2+}) and ferric (Fe^{3+}) salts, typically in a molar ratio of 1:2, are dissolved in deionized water under an inert or mildly acidic environment to prevent premature oxidation of Fe^{2+} ions. Common precursors include $\text{FeCl}_2 \cdot 4\text{H}_2\text{O}$ and $\text{FeCl}_3 \cdot 6\text{H}_2\text{O}$. The solution is heated (usually 60–80 °C) under continuous stirring to ensure homogeneity. A strong base such as NaOH or NH_4OH is then added dropwise, leading to a rapid increase in pH (around 9–11), which initiates the nucleation and growth of Fe_3O_4 nanoparticles.

The formation of magnetite nanoparticles occurs according to the following reaction: $Fe^{2+} + 2Fe^{3+} + 8OH^{-} \rightarrow Fe_3O_4 + 4H_2O$
 Upon addition of the base, a black precipitate of Fe_3O_4 forms almost instantly, indicating successful nucleation. The reaction conditions, such as pH, temperature, ionic strength, and stirring rate, play a critical role in controlling particle size, distribution, and crystallinity. Higher pH and temperature generally promote faster nucleation, leading to smaller particle sizes, while controlled addition of base helps in achieving uniform morphology. After synthesis, the nanoparticles are separated using magnetic decantation or centrifugation, followed by repeated washing with deionized water and ethanol to remove unreacted ions and impurities. The purified nanoparticles are then dried under vacuum or mild heating.

The synthesized Fe_3O_4 nanoparticles typically exhibit superparamagnetic behavior at nanoscale dimensions, which is highly desirable for biomedical applications. Superparamagnetism ensures that the nanoparticles show strong magnetization under an external magnetic field but negligible remanence after removal of the field, thereby preventing aggregation in physiological environments. Additionally, these nanoparticles possess good biocompatibility, high surface area, and excellent magnetic responsiveness, making them suitable for applications such as targeted drug delivery, magnetic hyperthermia, and actuation in magnetic hydrogel microrobots.

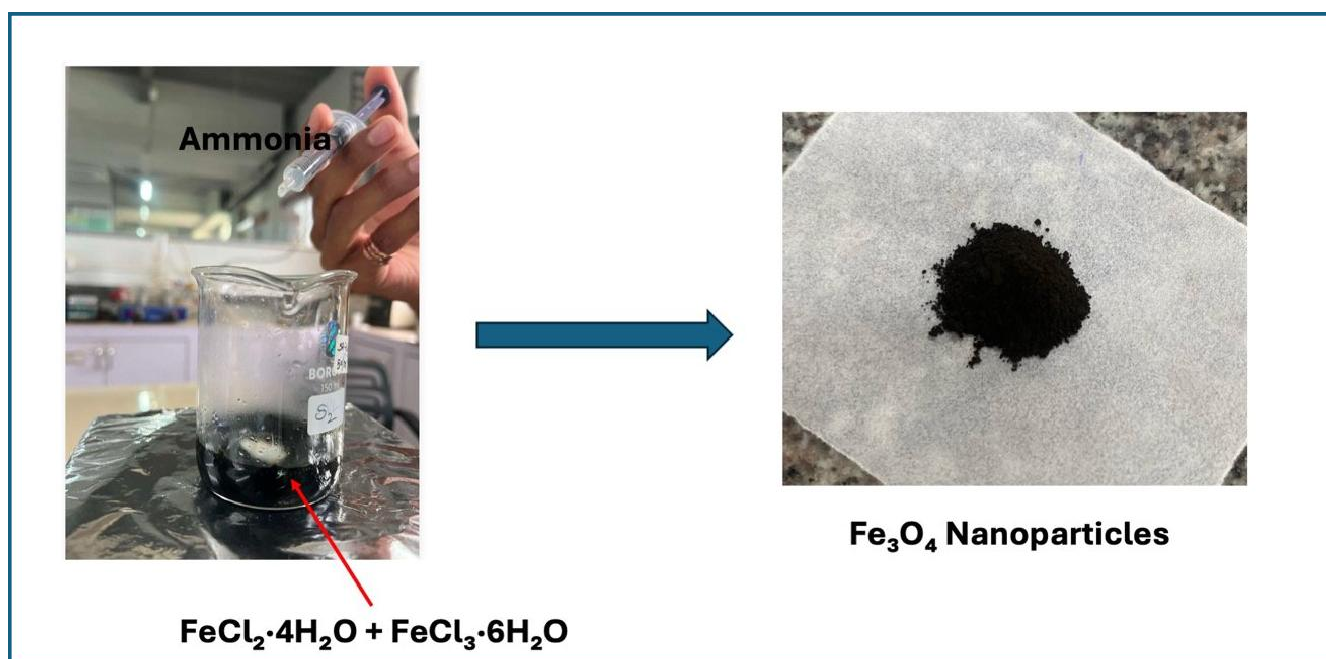


Figure No. 4.2: Synthesis of Iron Oxide nanoparticles.

Table No. 4.1: Quantity of Materials Used for Reaction

Sr. No	Materials	Concentration	Quantity
1	$FeCl_3$	0.1M	0.162 gm
2	$FeCl_2$	0.05M	0.063 gm
3	DDW (Double Distilled Water)	-	10 ml
4	Ammonia	0.05M	Adding Dropwise until black precipitation

4.2 Preparation of PVA-Gelatin Hydrogel (Freeze-Thaw and Crosslinking)

A PVA–gelatin hydrogel matrix is prepared by dissolving polyvinyl alcohol (PVA) and gelatin separately in distilled water under continuous stirring at elevated temperature to ensure complete dissolution and formation of homogeneous polymer solutions. PVA typically requires heating (~80–90 °C) to dissolve fully due to its semi-crystalline nature, while gelatin dissolves at comparatively lower temperatures (~40–50 °C). The two solutions are then mixed thoroughly in desired ratios to obtain a uniform polymer blend. The presence of hydroxyl groups in PVA and amino/carboxyl groups in gelatin facilitates intermolecular interactions such as hydrogen bonding, which is essential for forming a stable hydrogel network. The mixed solution is subjected to repeated freeze–thaw cycles, which play a crucial role in physical crosslinking. During freezing, water molecules crystallize and phase separation occurs, forcing PVA chains to align and form crystalline microdomains that act as physical crosslinking points. Upon thawing, the ice melts but the crystalline regions remain intact, resulting in a physically crosslinked network. Repetition of these cycles enhances the degree of crystallinity, thereby improving the mechanical strength, elasticity, and structural stability of the hydrogel without the need for toxic chemical crosslinkers. This method is particularly advantageous for biomedical applications as it preserves biocompatibility.

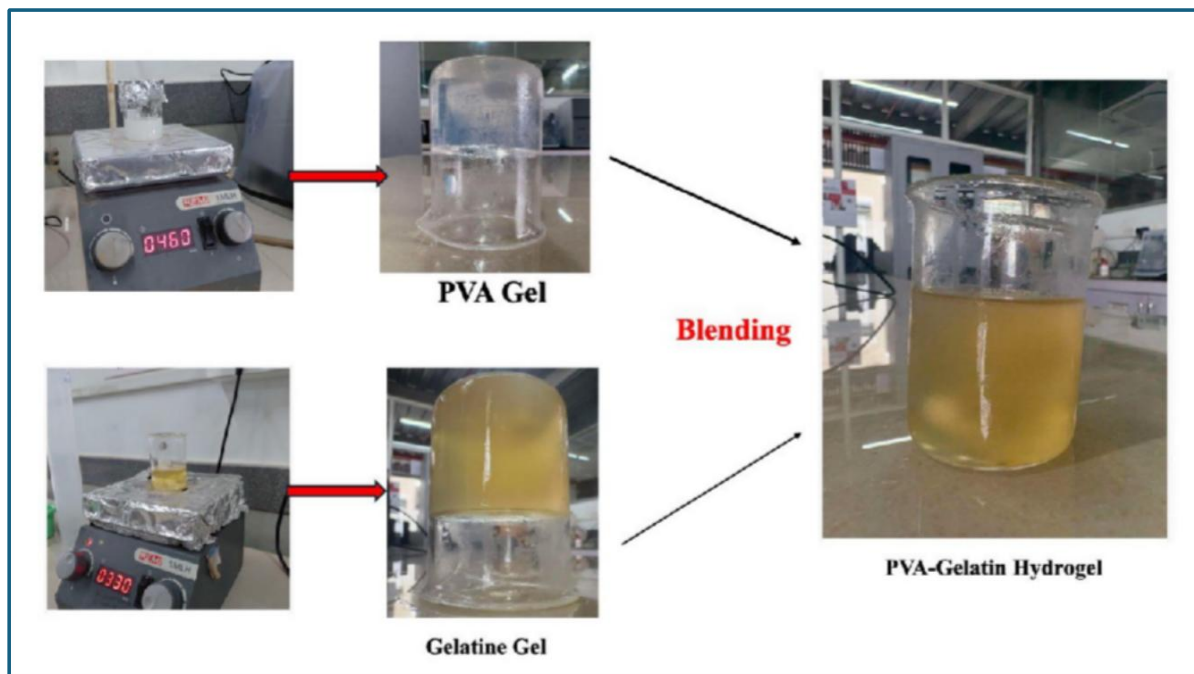


Figure No. 4.3: Synthesis of PVA-Gelatin hydrogel by Freeze-Thaw Cycle

To further enhance the mechanical robustness and durability of the hydrogel, chemical crosslinking agents such as glutaraldehyde or calcium chloride (CaCl_2) may be introduced.

Glutaraldehyde forms covalent bonds with amino groups of gelatin, strengthening the network, whereas Ca^{2+} ions can induce ionic crosslinking (especially in systems containing functional groups capable of coordination), contributing to improved rigidity and stability. The combination of physical and chemical crosslinking results in a dual-network hydrogel with superior mechanical integrity, controlled swelling behavior, and resistance to degradation. The resulting PVA–gelatin hydrogel exhibits a flexible, porous, and biocompatible three-dimensional structure capable of encapsulating nanoparticles and bioactive molecules. Its high absorption capacity and tissue-like mechanical properties make it suitable for mimicking biological environments. Moreover, the interconnected porous network facilitates diffusion-controlled transport, which is essential for applications such as drug delivery, tissue engineering, and magnetic microrobotics. This hydrogel matrix thus serves as an ideal platform for incorporating functional nanoparticles while maintaining structural stability and biological compatibility.

Table No. 4.2: Quantity of Materials Used for Synthesis

Sr. No	Materials	Concentration	Quantity
1	PVA (Polyvinyl Alcohol)	30%	7.5gm
2	Gelatin	15%	3.75gm
3	DDW (Double Distilled Water)	-	25ml
4	Fe ₃ O ₄ nanoparticles	-	Added during stirring

4.3 Incorporation of Fe₃O₄ Nanoparticles into Hydrogel (Fabrication of Magnetic Microrobots)

To prepare magnetic hydrogel microrobots, the synthesized Fe₃O₄ nanoparticles are incorporated into a polyvinyl alcohol (PVA)–gelatin hydrogel matrix during the gelation process, ensuring homogeneous dispersion within the three-dimensional polymeric network. PVA provides excellent film-forming ability, mechanical strength, and flexibility, while gelatin contributes biocompatibility and bioactive functional groups that enhance cell interaction and biodegradability. The interaction between PVA and gelatin, often facilitated through physical crosslinking (freeze–thaw cycles) or chemical crosslinking, leads to the formation of a stable interpenetrating network (IPN). During this stage, Fe₃O₄ nanoparticles become embedded within the hydrogel matrix through hydrogen bonding and physical entrapment, preventing aggregation and ensuring uniform magnetic properties throughout the structure.

The uniform distribution of Fe₃O₄ nanoparticles is critical, as it directly influences the magnetic responsiveness and actuation efficiency of the resulting microrobots. When subjected to an external magnetic field, these nanoparticles generate magnetic forces and torques, enabling controlled movement, rotation, or deformation of the hydrogel structure. By tuning parameters such as nanoparticle concentration, crosslinking density, and hydrogel geometry, the mechanical stiffness, swelling behavior, and responsiveness of the system can be precisely controlled. This allows the fabrication of microrobots with tailored properties, including shape morphing, directional locomotion, and responsiveness to alternating magnetic fields (AMF).

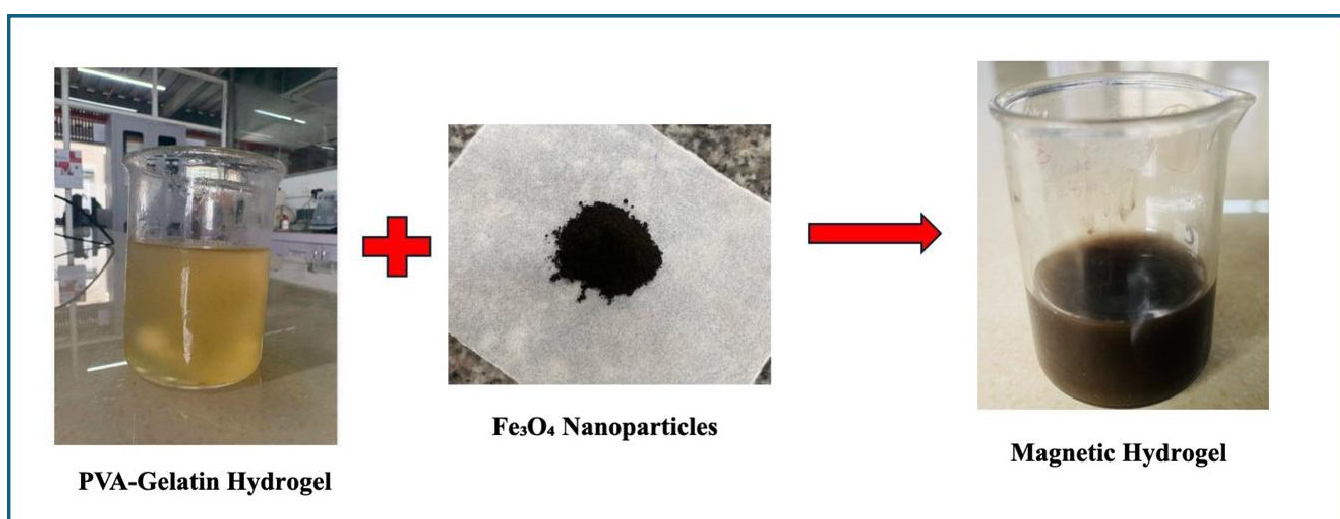


Figure No. 4.4: Incorporation of fe3O4 nanoparticles within PVA-Gelatin hydrogel to form magnetic hydrogel.

4.4 Fabrication of flower-shaped magnetic hydrogel microrobot using mould-assisted freeze–thaw method at $-20\text{ }^{\circ}\text{C}$.

After the successful preparation of the magnetic hydrogel precursor, consisting of a PVA–gelatin matrix uniformly incorporated with Fe_3O_4 nanoparticles, the mixture is carefully poured into a predefined mould to obtain the desired microrobot geometry. The mould plays a crucial role in determining the shape, surface morphology, and structural uniformity of the final hydrogel construct. In this work, a flower-shaped mould is selected to fabricate biomimetic microrobots, as such geometries provide a higher surface-to-volume ratio and structural symmetry. These characteristics are advantageous for enhancing interaction with surrounding fluids, improving propulsion efficiency, and enabling better control under external magnetic fields. Once the hydrogel solution is cast into the mould, it is subjected to a controlled freezing process at $-20\text{ }^{\circ}\text{C}$ and maintained overnight. This step is essential for inducing physical crosslinking within the polymer network. During freezing, water molecules crystallize into ice, leading to phase separation between polymer-rich and solvent-rich regions. This phenomenon promotes the alignment and aggregation of PVA chains, resulting in the formation of crystalline microdomains that act as physical crosslinking points. Simultaneously, gelatin interacts with PVA through hydrogen bonding and intermolecular interactions, further strengthening and stabilizing the three-dimensional network. The freezing conditions, including temperature and duration, significantly influence the pore structure, crosslinking density, and mechanical strength of the hydrogel.

During this process, the Fe_3O_4 nanoparticles become effectively immobilized within the polymer matrix through physical entrapment and interfacial interactions. The rapid solidification prevents nanoparticle aggregation and sedimentation, ensuring their uniform distribution throughout the hydrogel network. This homogeneous dispersion is critical for achieving consistent magnetic properties, which directly affect the actuation efficiency and controllability of the microrobot under external magnetic fields. After complete freezing, the hydrogel is allowed to thaw at room temperature. The melting of ice crystals results in the formation of an interconnected porous structure while preserving the physically crosslinked network. Consequently, the hydrogel retains the exact shape of the mould, producing a well-defined flower-shaped magnetic hydrogel microrobot. The porous architecture enhances swelling behavior, facilitates diffusion of molecules, and provides space for drug loading, while the polymer network ensures flexibility, elasticity, and mechanical stability.

Furthermore, the presence of Fe_3O_4 nanoparticles imparts magnetic responsiveness to the hydrogel, allowing remote actuation and navigation using external magnetic fields. Under static magnetic fields, the microrobot can exhibit controlled translational and rotational motion, while under alternating magnetic fields, it can generate localized heat suitable for magnetic hyperthermia applications. The flower-like geometry also contributes to improved hydrodynamic behavior and directional control in fluidic environments. Overall, such shape-engineered magnetic hydrogel microrobots demonstrate significant potential for advanced biomedical applications, including targeted drug delivery, localized therapy, and minimally invasive treatment strategies.

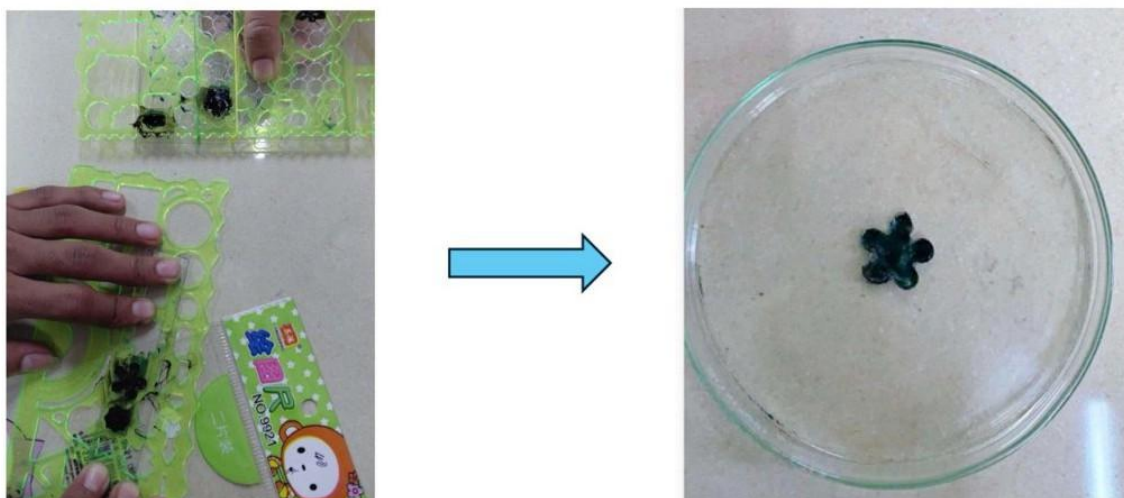


Figure No. 4.5: Shape morphing of Hydrogel



Figure No. 4.6: Measurement of Wet and Dry Microrobot and Different shapes of Microrobot

Table No. 4.3: Experimental Synthesis

Sr.No.	Steps	Experimental Procedure	Conditions
1	I	Dissolution of PVA in distilled water under magnetic stirring	80–90°C for 1–2 hr
2	II	Preparation of gelatin solution	40–50°C with continuous stirring
3	III	Mixing of PVA and gelatin solution	Constant stirring for 30–60 min
4	IV	Addition of Fe ₃ O ₄ nanoparticles into polymer mixture	Ultrasonication and stirring
5	V	Homogeneous dispersion of nanoparticles	20–30 min ultrasonication
6	VI	Pouring solution into mold/template	At Room temperature
7	VII	Crosslinking of hydrogel structure	Freeze-thaw cycles / chemical treatment
8	VIII	Drying and removal of synthesized microrobot	Ambient drying
9	IX	Characterization using FTIR, XRD	Structural and magnetic analysis

ANALYSIS

5.1 XRD

X-ray diffraction (XRD) is a fundamental characterization technique used to analyze the internal structure of crystalline materials. It is based on the interaction of X-rays with the periodic arrangement of atoms in a crystal lattice. When monochromatic X-rays are incident on a crystalline sample, they are scattered by the electrons of the atoms. Due to the regular arrangement of atoms, these scattered waves interfere constructively at specific angles, producing diffraction peaks. This phenomenon follows Bragg's law, which relates the angle of diffraction to the spacing between atomic planes. As a result, XRD provides indirect but highly reliable information about how atoms are arranged inside a material, making it an essential tool in physics, chemistry, and materials science. The XRD pattern is typically represented as a graph of intensity versus diffraction angle (2θ). Each peak in the pattern corresponds to a specific set of atomic planes within the crystal. The position of these peaks depends on the interplanar spacing, while the intensity is influenced by the type and arrangement of atoms. Because every crystalline material has a unique atomic structure, it produces a characteristic diffraction pattern that can be used as a fingerprint for phase identification. By comparing experimental data with standard reference databases, one can determine whether the material is pure or contains multiple phases. This makes XRD extremely useful for confirming successful synthesis and detecting impurities.

An important concept in XRD analysis is the Miller indices, denoted as (hkl), which represent the orientation of crystallographic planes in a crystal lattice. These indices are a set of three integers that describe how a plane intersects the crystallographic axes. For example, a (100) plane intersects the x-axis but is parallel to the y- and z-axes, while a (111) plane intersects all three axes equally. Each (hkl) plane has a specific interplanar spacing, and therefore produces a diffraction peak at a particular angle. By identifying these planes in an XRD pattern, one can determine the crystal structure of the material, such as cubic, tetragonal, or hexagonal. The indexing of peaks with (hkl) values is a key step in structural analysis. Another important aspect of XRD is the information it provides about crystallinity and crystallite size. Sharp and well-defined peaks indicate a highly crystalline material with long-range atomic order, whereas broad peaks suggest smaller crystallite size or partial amorphous

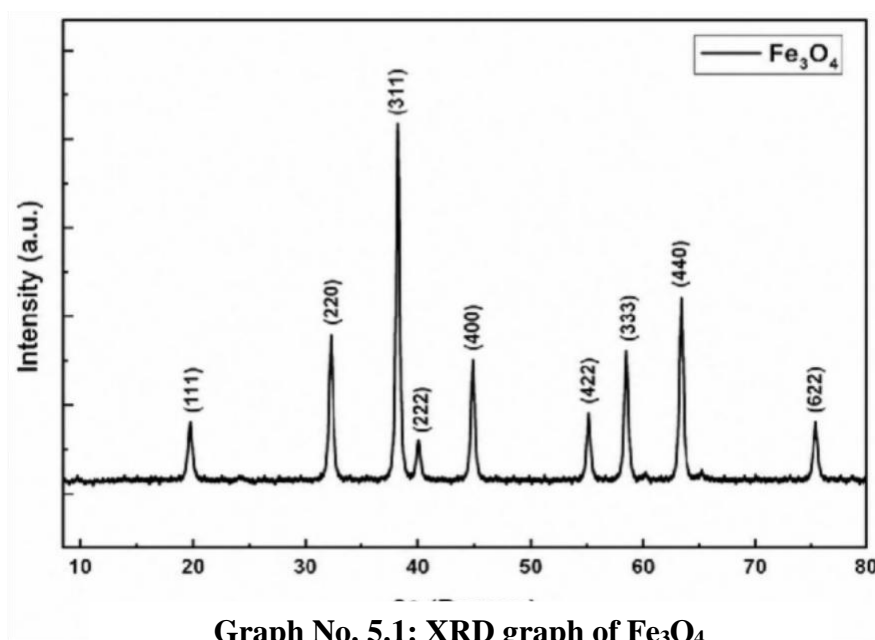
nature. In nanomaterials, peak broadening is commonly observed due to the reduced size of crystalline domains. This broadening can be quantitatively analyzed using the Debye–Scherrer equation to estimate the average crystallite size. Additionally, shifts in peak positions can indicate lattice strain, defects, or changes in composition, providing further insight into the material's structural properties.

Overall, XRD is a versatile and powerful technique that helps in understanding the relationship between structure and properties of materials. It allows researchers to identify phases, determine crystal structures, analyze crystallinity, and estimate particle size, all from a single measurement. For students, it is important to recognize that XRD does not provide a direct image of atoms, but rather a diffraction pattern that must be interpreted using physical principles. Mastering concepts such as Bragg's law, peak indexing, and Miller indices (hkl) is essential for correctly analyzing XRD data and applying it to real-world materials research and development.

The X-ray diffraction (XRD) pattern of the synthesized Fe_3O_4 nanoparticles confirms the formation of a crystalline magnetite phase with a face-centered cubic (fcc) spinel structure. The diffraction peaks observed at 2θ values around $\sim 30^\circ$, 35° , 43° , 53° , 57° , and 62° correspond to the crystallographic planes indexed as (220), (311), (400), (422), (511)/(333), and (440), respectively. Among these, the most intense peak at $\sim 35^\circ$ corresponding to the (311) plane is a characteristic signature of Fe_3O_4 . The presence of these well-defined peaks and their agreement with standard JCPDS data (card no. 19-0629) confirm the successful synthesis of magnetite nanoparticles without the formation of secondary impurity phases such as hematite (Fe_2O_3). The sharpness and intensity of the diffraction peaks indicate good crystallinity of the synthesized nanoparticles. The broadening of peaks, particularly at higher angles, suggests that the particles are in the nanoscale range. The average crystallite size can be estimated using the Debye–Scherrer equation based on the full width at half maximum (FWHM) of the most intense peak (311). The calculated crystallite size typically falls within the nanometer range, which is consistent with the expected size for magnetic nanoparticles synthesized via the co-precipitation method.

Furthermore, the absence of extra peaks in the XRD pattern confirms the phase purity of the Fe₃O₄ nanoparticles. The crystalline nature and nanoscale size are crucial for their magnetic properties, particularly superparamagnetic behavior, which is essential for

applications such as magnetic hyperthermia, targeted drug delivery, and actuation in magnetic hydrogel microrobots. Overall, the XRD analysis validates the successful synthesis of pure, crystalline Fe₃O₄ nanoparticles suitable for biomedical and microrobotic applications.



Graph No. 5.1: XRD graph of Fe₃O₄

Table No. 5.1: Graphical Data of Fe₃O₄

Sr No.	Sample	Peaks	Wavenumber(cm ⁻¹)
1	Fe ₃ O ₄	111	~18
2		220	~30
3		311	~35
4		222	~37
5		400	~43
6		422	~53
7		333	~57
8		440	~62
9		622	~74

5.2 FTIR Study

Fourier Transform Infrared (FT-IR) spectroscopy is a widely used analytical technique for identifying chemical structures and functional groups in a material. It is based on the interaction between infrared radiation and matter, where molecules absorb specific frequencies of IR light corresponding to the vibrations of their chemical bonds. When IR radiation passes through a sample, certain wavelengths are absorbed while others are transmitted, producing a spectrum that represents the molecular fingerprint of the material. Each type of chemical bond (such as O–H, C=O, N–H, etc.) vibrates at characteristic frequencies, allowing FT-IR to be used for qualitative identification of compounds. An FT-IR spectrum is typically presented as a plot of transmittance (or absorbance) versus wavenumber (cm^{-1}). The wavenumber range usually extends from 4000 to 400 cm^{-1} , covering different regions associated with various molecular vibrations. The region from 4000–1500 cm^{-1} is known as the functional group region, where most characteristic bond vibrations appear, while the region below 1500 cm^{-1} is called the fingerprint region, which is highly specific to individual compounds. Peaks in the spectrum correspond to absorption of IR radiation, and their position, shape, and intensity provide detailed information about the molecular structure and interactions within the sample.

FT-IR spectroscopy is particularly useful for identifying functional groups and studying chemical bonding in polymers, biomolecules, and nanomaterials. For example, broad peaks around 3200–3500 cm^{-1} typically indicate O–H or N–H stretching vibrations, while sharp peaks near 1700 cm^{-1} correspond to C=O stretching. Similarly, peaks in the range of 1000–1300 cm^{-1} are often associated with C–O or C–N stretching. By analyzing these peaks, one can confirm the presence of specific chemical groups, detect chemical modifications, and study interactions such as hydrogen bonding between different components in a composite material. Another important advantage of FT-IR is its ability to monitor chemical changes and interactions in materials. For instance, shifts in peak positions, changes in intensity, or the appearance/disappearance of peaks can indicate chemical reactions, crosslinking, or interactions between different components. In composite systems, such as polymer–nanoparticle materials, FT-IR helps confirm successful incorporation and interaction between phases. It can also provide insight into the stability and compatibility of materials, which is essential for applications in drug delivery, tissue engineering, and other biomedical fields.

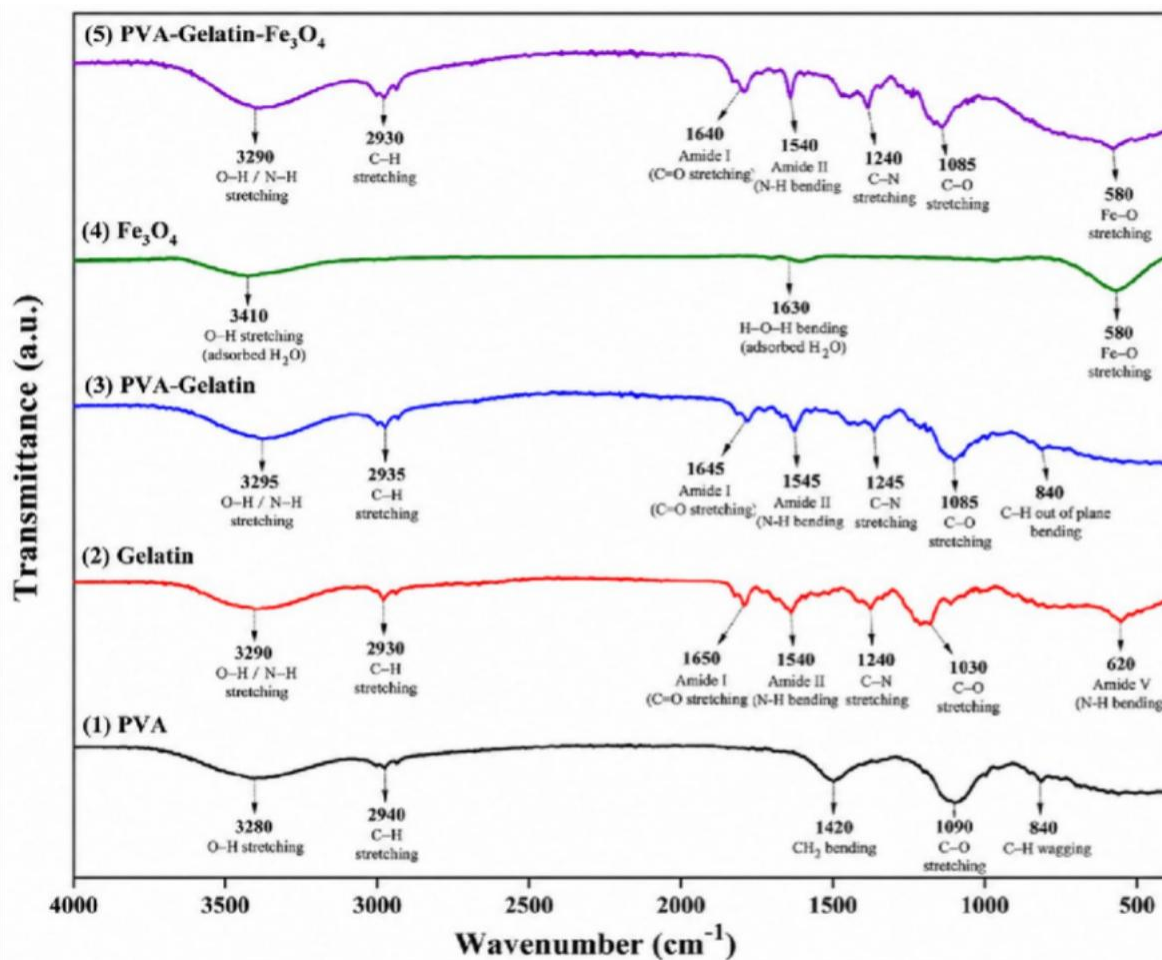
Overall, FT-IR is a rapid, non-destructive, and highly informative technique that plays a crucial role in material characterization. It provides valuable information about molecular structure, functional groups, and chemical interactions, making it indispensable in research and industry. For students, it is important to understand that FT-IR does not give a direct image of molecules but provides spectral data that must be interpreted based on known vibrational frequencies. Mastery of FT-IR analysis enables accurate identification of materials and a deeper understanding of their chemical behaviour and properties.

The FT-IR spectra presented in the figure confirm the successful formation of the PVA–gelatin hydrogel and its subsequent incorporation with Fe_3O_4 nanoparticles. The spectrum of pure PVA shows a broad peak around $\sim 3280 \text{ cm}^{-1}$ corresponding to O–H stretching vibrations, along with peaks near $\sim 2940 \text{ cm}^{-1}$ due to C–H stretching, and $\sim 1090 \text{ cm}^{-1}$ attributed to C–O stretching. In the case of gelatin, characteristic peaks are observed at $\sim 3290 \text{ cm}^{-1}$ (O–H/N–H stretching), $\sim 1650 \text{ cm}^{-1}$ (amide I, C=O stretching), and $\sim 1540 \text{ cm}^{-1}$ (amide II, N–H bending), confirming its protein structure.

In the PVA–gelatin composite spectrum, the main peaks from both polymers are retained but show slight shifts in position and intensity, particularly in the O–H/N–H and amide regions. This indicates strong intermolecular interactions, mainly hydrogen bonding, between PVA and gelatin chains, confirming the formation of a blended hydrogel network. The presence of peaks around $\sim 1245 \text{ cm}^{-1}$ (C–N stretching) and $\sim 1085 \text{ cm}^{-1}$ (C–O stretching) further supports integration of both polymers into a single structure. Such interactions are essential for enhancing the mechanical strength and stability of the hydrogel.

In the spectrum of Fe_3O_4 nanoparticles, a characteristic peak is observed around $\sim 580 \text{ cm}^{-1}$ corresponding to Fe–O stretching vibrations, confirming the formation of magnetite. Additionally, weak bands around $\sim 3410 \text{ cm}^{-1}$ and $\sim 1630 \text{ cm}^{-1}$ are attributed to O–H stretching and H–O–H bending of adsorbed water molecules. In the final PVA–gelatin– Fe_3O_4 composite, the presence of this Fe–O peak along with the polymer peaks confirms the successful

incorporation of magnetic nanoparticles into the hydrogel matrix. The slight change in peak positions and intensities further indicate interaction between the nanoparticles and polymer network, demonstrating the formation of a stable magnetic hydrogel suitable for biomedical and microbotic applications. Top of FormBottom of Form



Graph No. 5.2: FTIR spectra of PVA, Gelatin, Fe₃O₄ and PVA-Gelatin- Fe₃O₄ composite

Table No. 5.2: Graphical Data of PVA

Sr No.	Sample	Peaks	Wavenumber(cm ⁻¹)
1	PVA	O-H stretching	3280
2		C-H stretching	2940
3		CH ₂ bending	1420
4		C-O stretching	1090
5		C-H wagging	840

Table No. 5.3: Graphical Data of Gelatin

Sr No.	Sample	Peaks	Wavenumber(cm ⁻¹)
1	Gelatin	O–H / N–H stretching	3290
2		C–H stretching	2930
3		Amide I (C=O stretching)	1650
4		Amide II (N–H bending)	1540
5		C–N stretching	1240
6		C–O stretching	1030
7		Amide V (N–H bending)	620

Table No. 5.4: Graphical Data of Fe₃O₄

Sr No.	Sample	Peaks	Wavenumber(cm ⁻¹)
1	Fe ₃ O ₄	O–H stretching (adsorbed H ₂ O)	3410
2		H-O-H bending (adsorbed H ₂ O)	1630
3		Fe–O stretching	580

Table No. 5.5: Graphical Data of PVA-Gelatin

Sr No.	Sample	Peaks	Wavenumber(cm ⁻¹)
1	PVA-Gelatin	O-H / N-H stretching	3295
2		C-H stretching	2935
3		Amide I (C=O stretching)	1645
4		Amide II (N-H bending)	1545
5		C-N stretching	1245
6		C-O stretching	1085
7		C-H out-of-plane bending	840

Table No. 5.6: Graphical Data of PVA-Gelatin- Fe₃O₄

Sr No.	Sample	Peaks	Wavenumber(cm ⁻¹)
1	PVA-Gelatin- Fe ₃ O ₄	O-H / N-H stretching	3290
2		C-H stretching	2930
3		Amide I (C=O stretching)	1640
4		Amide II (N-H bending)	1540
5		C-N stretching	1240
6		C-O stretching	1085
7		Fe-O stretching	580

5.3 Induction heating Study :

An induction heating system is a non-contact method of generating heat within a material using electromagnetic induction. It operates on the principle that when an alternating current (AC) passes through a coil (induction coil), it produces a time-varying magnetic field around it. When a conductive material—such as magnetic nanoparticles or a metal—is placed within this magnetic field, electric currents known as eddy currents are induced inside the material. These currents encounter resistance within the material, leading to the generation of heat. In magnetic materials, additional heat is produced due to magnetic losses such as hysteresis loss and relaxation mechanisms, making the heating process highly efficient. In biomedical applications, particularly for magnetic hydrogels or nanoparticles, induction heating is typically achieved using an alternating magnetic field (AMF). When Fe₃O₄ nanoparticles are exposed to an AMF, heat is generated through Néel relaxation (internal magnetic moment flipping) and

Brownian relaxation (physical rotation of particles), along with minor hysteresis losses depending on particle size. The amount of heat generated depends on several factors, including magnetic field strength, frequency, particle size, and concentration of nanoparticles. This localized heating capability is especially useful in applications like magnetic hyperthermia, where cancer cells can be selectively destroyed by raising the temperature to a therapeutic range (typically 42–45 °C).

One of the major advantages of induction heating systems is their ability to provide rapid, uniform, and controllable heating without direct contact. This makes them highly suitable for sensitive applications such as drug delivery and targeted therapy. In magnetic hydrogel microrobots, induction heating can be used not only for therapeutic purposes but also to trigger controlled drug release by altering the hydrogel structure. Overall, induction heating systems offer precise control, high efficiency, and minimal damage to surrounding tissues, making them a powerful tool in advanced biomedical and nanotechnology applications.

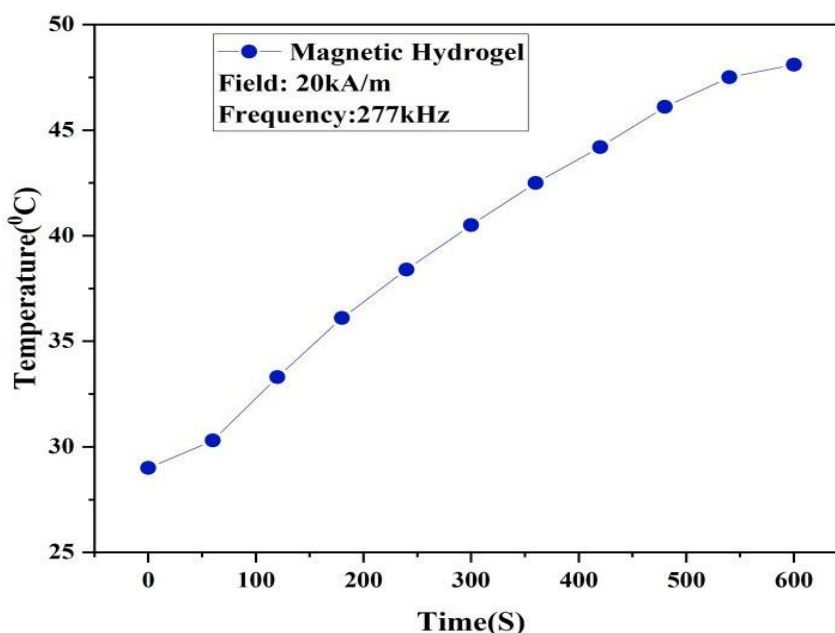
The shown setup is an induction heating system used to generate heat through electromagnetic induction without direct contact. It consists of a power supply unit, control panel, and an induction coil connected through cooling lines. When alternating current flows through the coil, it produces a rapidly changing magnetic field, which induces eddy currents in nearby conductive or magnetic materials. These currents generate heat due to electrical resistance, while magnetic materials such as Fe₃O₄ nanoparticles additionally produce heat through magnetic losses. The system allows precise control of parameters like power, frequency, and time, enabling uniform and rapid heating. Such induction heating systems are widely used in research and biomedical applications, including magnetic hyperthermia and controlled drug release, where localized and efficient heating is required.



Figure No. 5.1: Induction Heating System

The graph represents the induction heating behavior of the magnetic hydrogel under an alternating magnetic field with a field strength of 20 kA/m and a frequency of 277 kHz. The temperature of the hydrogel increases steadily with time, starting from around 29 °C and reaching approximately 48 °C within 600 seconds. This rise in temperature confirms the effective heat generation capability of the embedded Fe₃O₄ nanoparticles when exposed to the alternating magnetic field. The initial gradual increase is followed by a more consistent rise, indicating efficient conversion of magnetic energy into thermal energy. The heating mechanism is mainly attributed to magnetic losses such as Néel and Brownian relaxation of the Fe₃O₄ nanoparticles present within the hydrogel matrix. As the magnetic field oscillates, the magnetic moments of the nanoparticles continuously realign, generating heat. The porous and hydrated structure of the hydrogel facilitates uniform heat distribution, resulting in a smooth and controlled temperature increase. The absence of sudden spikes in the curve indicates stable and uniform heating behavior throughout the duration of the experiment.

Importantly, the temperature reaches the therapeutic range of approximately 42–45 °C, which is suitable for magnetic hyperthermia applications. This demonstrates that the prepared magnetic hydrogel is capable of generating sufficient localized heat for potential cancer treatment without exceeding harmful temperature limits. Therefore, the graph confirms the suitability of the magnetic hydrogel system for biomedical applications such as controlled hyperthermia and stimuli-responsive drug delivery.



Graph No. 5.3: Hyperthermia of Magnetic Hydrogel

Table No. 5.7: Graphical Data of Magnetic Hydrogel

Sr No.	Sample	Time (s)	Temperature °C
1	Magnetic Hydrogel	0	29
2		60	30
3		120	33
4		180	36
5		240	38.5
6		300	40.5

7	360	42.5
8	420	44
9	480	46
10	540	47.5
11	600	48

5.4 Electromagnetic Solenoid Coil :

The experimental setup shown is an induction heating system, which is widely used in laboratories and industries for rapid and controlled heating of conductive materials. This system mainly consists of an induction power supply unit, an induction coil (work coil), a cooling system, and a sample holder or crucible. The induction coil, made of copper tubing, is connected to the power supply and is usually cooled by circulating water through it to prevent overheating. The sample to be heated is placed inside or near the coil, often supported by a refractory or insulating material that can withstand high temperatures. The entire setup is designed to provide efficient, localized heating without direct contact between the heat source and the material



Figure No. 5.2: Electromagnetic Solenoid Coil

The working principle of this system is based on the concept of electromagnetic induction, which is a fundamental principle in physics. When high-frequency alternating current passes through the induction coil, it generates a rapidly changing magnetic field around the coil. According to Faraday's law of electromagnetic induction, this varying magnetic field induces electric currents, known as eddy currents, in any conductive material placed within the field. These eddy currents flow through the material and,

due to the electrical resistance of the material, produce heat. This phenomenon is called Joule heating or resistive heating. The amount of heat generated depends on factors such as the electrical conductivity, magnetic permeability, size, and shape of the material, as well as the frequency of the current.

One of the key observations in this experiment is that the heating is highly localized and concentrated at specific regions of the sample. As seen in the setup, the center portion of the material shows signs of intense heating, often appearing darkened or burnt. This occurs because the magnetic field is strongest near the center of the coil, leading to higher induced currents in that region. Additionally, if the material is ferromagnetic, hysteresis losses also contribute to heating, especially at lower temperatures. As the temperature increases, the material may lose its magnetic properties, and eddy current heating becomes dominant.

The induction coil used in this setup is often referred to in physics as a type of solenoid, as it consists of a coiled conductor that produces a magnetic field when current flows through it. However, unlike a simple solenoid, the induction coil is specifically designed to operate at high frequencies and is shaped to provide uniform and efficient heating. In this case, the coil appears to be a flat or pancake-type coil, which is commonly used for surface heating applications. The use of copper as the coil material is due to its excellent electrical conductivity, which minimizes energy loss and improves efficiency.

The cooling system, typically consisting of water flowing through flexible tubes, plays a crucial role in maintaining the performance and safety of the setup. Since high currents are used, the coil can heat up significantly, and without proper cooling, it may get damaged or lose efficiency. The continuous flow of water removes excess heat and ensures stable operation. The insulating materials used in the setup help to reduce heat loss to the surroundings and protect the supporting structures from high temperatures.

Induction heating offers several advantages over conventional heating methods. It is a non-contact process, which means there is no direct flame or physical contact with the material, resulting in a cleaner and safer operation. It provides rapid heating, high efficiency, and precise control over temperature and heating area. These features make it highly suitable for applications such as metal melting, heat treatment processes like hardening and annealing, brazing, soldering, and various laboratory experiments involving material testing.

In conclusion, the induction heating setup demonstrates an efficient and modern method of heating materials using the principle of electromagnetic induction. It highlights important physical concepts such as eddy currents, Joule heating, and magnetic field generation. The system is not only useful for academic experiments but also has significant industrial applications due to its speed, efficiency, and control. This experiment helps in understanding how electrical energy can be converted into heat energy in a controlled and contactless manner, making it an important topic in the field of applied physics and engineering.

5.5 Magnetic Response study :

The magnetic field response study of the fabricated magnetic hydrogel microrobots was carried out by immersing them in a phosphate-buffered saline (PBS) solution to simulate a physiological environment. PBS is commonly used because it maintains a stable pH and ionic strength similar to biological fluids, ensuring that the behavior of the microrobots can be evaluated under realistic conditions. In this setup, the microrobots were placed inside a petri dish containing PBS, and an external magnetic field was applied using a permanent magnet brought close to the system.

Upon application of the magnetic field, the microrobots exhibited a clear and immediate response, demonstrating their magnetic sensitivity. The embedded Fe_3O_4 nanoparticles within the hydrogel matrix interact with the external magnetic field, generating magnetic forces that induce movement. As observed in the figure, the microrobot moves toward the direction of the

applied magnet, confirming successful magnetic actuation. The motion can include translation, rotation, or alignment depending on the orientation and strength of the magnetic field. This behavior indicates that the nanoparticles are well-dispersed within the hydrogel, allowing uniform magnetic responsiveness. The study also highlights the controllability of microrobot motion in a fluidic medium. By changing the position or orientation of the external magnet, the direction of movement of the microrobot can be precisely guided. This demonstrates that the system is capable of remote navigation, which is a key requirement for microrobotic applications. The response observed in PBS further confirms that the hydrogel maintains its structural integrity and functionality

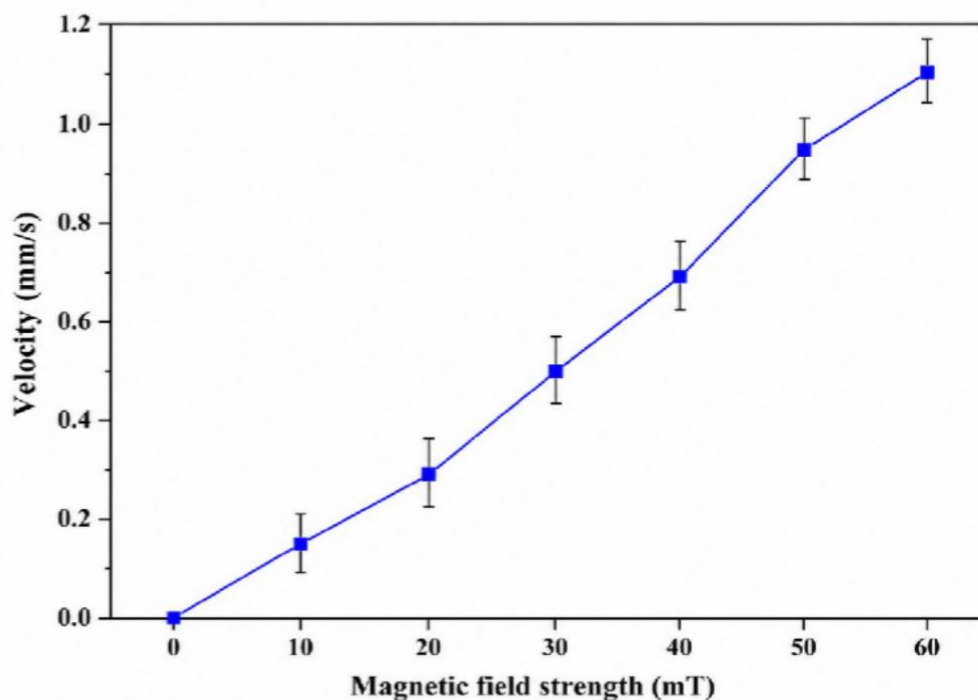
in aqueous environments, without degradation or loss of magnetic properties.

Additionally, the movement of the microrobots in PBS suggests low resistance and effective interaction with the surrounding medium. The soft and flexible nature of the hydrogel allows smooth motion without causing disturbance to the fluid environment. The responsiveness also indicates that sufficient magnetic force is generated to overcome viscous drag in the solution. This is particularly important for biomedical applications where microrobots need to travel through complex biological fluids. Overall, the magnetic field response study confirms that the fabricated magnetic hydrogel microrobots exhibit efficient, controllable, and stable motion under an external magnetic field in a physiological medium. This demonstrates their strong potential for applications such as targeted drug delivery, minimally invasive procedures, and micro-scale manipulation within biological systems.

Top of Form Bottom of Form

5.6 Magnetic Actuation Study :

Magnetic actuation study is used to evaluate how effectively a material or microrobot responds to an external magnetic field. In systems such as magnetic hydrogels, this behaviour is mainly due to the presence of magnetic nanoparticles like Fe_3O_4 embedded within the polymer matrix. When an external magnetic field is applied, these nanoparticles experience magnetic forces and torques, which induce motion or deformation in the material. The response can include translation (movement), rotation, or bending, depending on the field strength, direction, and the geometry of the microrobot. This allows remote, contactless control of the system. The study is typically performed by placing the magnetic sample in a medium such as water or buffer solution and applying a magnetic field using a permanent magnet or electromagnetic setup. The movement of the microrobot is recorded using a camera or microscope, and parameters such as displacement, velocity, and direction are analysed. By varying the magnetic field strength or position, researchers can study how the actuation behaviour changes. Graphs such as velocity vs magnetic field strength or displacement vs time are often used to quantify the performance. Magnetic actuation studies help in understanding the controllability, responsiveness, and efficiency of magnetic systems. These properties are essential for applications like targeted drug delivery, microfluidics, and soft robotics, where precise navigation and controlled motion are required. A good magnetic actuation system should show quick response, stable movement, and predictable behavior under different magnetic field conditions.



Graph No. 5.4: Strength graph of Magnetic Hydrogel

The presented graph illustrates the magnetic actuation behaviour of the hydrogel microrobot by plotting its velocity (mm/s) as a function of applied magnetic field strength (mT). To perform this actuation study, the fabricated magnetic hydrogel microrobot is placed in a fluid medium (such as water or buffer solution), and an external magnetic field is applied using a permanent magnet or an electromagnetic coil system. The strength of the magnetic field is gradually increased, and the motion of the microrobot is recorded using an optical microscope or camera setup. The displacement of the microrobot over time is measured, and its velocity is calculated. Multiple readings are typically taken at each magnetic field strength to ensure accuracy, which is why error bars are included in the graph.

The graph clearly shows that the velocity of the microrobot increases with increasing magnetic field strength. This behaviour occurs because higher magnetic field strength generates a greater magnetic force on the embedded Fe₃O₄ nanoparticles, resulting in stronger propulsion of the hydrogel structure. Initially, the increase in velocity is gradual, but as the field strength continues to rise, the microrobot exhibits a more significant increase in speed due to enhanced magnetic torque and force overcoming viscous resistance of the surrounding fluid. The nearly linear trend observed in the graph indicates efficient and predictable magnetic responsiveness of the microrobot.

Overall, this graph confirms that the fabricated magnetic hydrogel microrobot exhibits effective magnetic actuation and controllable motion under an external magnetic field. The presence of small error bars suggests good reproducibility and stability of the system. Such behaviour is essential for practical biomedical applications, where precise control over microrobot movement is required for targeted drug delivery, navigation in biological fluids, and minimally invasive therapeutic procedures

RESULT AND DISCUSSION

The successful fabrication of the PVA–gelatin–Fe₃O₄ magnetic hydrogel microrobot was confirmed through structural and chemical characterization studies. FT-IR analysis verified the presence of characteristic functional groups of PVA, gelatin, and Fe₃O₄ nanoparticles, indicating successful incorporation and intermolecular interactions within the hydrogel matrix. XRD analysis confirmed the crystalline spinel structure of Fe₃O₄ nanoparticles with good phase purity and crystallinity, while the freeze–thaw process produced a stable and porous hydrogel network suitable for biomedical applications.

Magnetic actuation and field response studies demonstrated that the fabricated microrobot exhibited efficient and controllable motion under external magnetic fields. The embedded Fe₃O₄ nanoparticles enabled remote locomotion, directional navigation, and magnetic responsiveness in PBS medium, confirming uniform nanoparticle dispersion and stable hydrogel integrity. The actuation graph showed that microrobot velocity increased with increasing magnetic field strength, indicating strong magnetic sensitivity and effective magnetic control.

Induction heating and magnetic hyperthermia studies revealed that the magnetic hydrogel generated localized heat under an alternating magnetic field, with the temperature increasing from room temperature to the therapeutic hyperthermia range (42–45 °C). This heating behavior confirmed the efficient magnetic-to-thermal energy conversion capability of Fe₃O₄ nanoparticles through Néel and Brownian relaxation mechanisms. The combined properties of biocompatibility, magnetic actuation, and controlled heat generation demonstrate the strong potential of the developed magnetic hydrogel microrobot for targeted cancer hyperthermia therapy, and minimally invasive biomedical applications.

FUTURESCOPE

The future scope of magnetically actuated hydrogel microrobots is highly promising due to their multifunctional capabilities and potential to revolutionize modern healthcare systems. Future research is expected to focus on improving navigation accuracy, miniaturization, biocompatibility, and intelligent control systems for better therapeutic performance. Researchers are working on integrating artificial intelligence and machine learning with magnetic actuation systems to achieve autonomous movement of microrobots within complex biological environments. Such advancements will allow precise targeting of diseased tissues, efficient drug delivery, and real-time monitoring of treatment processes. In cancer therapy, future hydrogel microrobots may combine hyperthermia treatment, controlled drug release, and biosensing within a single platform, thereby improving treatment effectiveness and reducing side effects associated with conventional therapies.

Another important future direction is the development of biodegradable and stimuli-responsive microrobots that can safely

dissolve inside the body after completing their function. This would eliminate the need for surgical removal and improve patient safety. Advanced fabrication methods such as 3D micro-printing, lithography, and nano-patterning are expected to improve the structural precision and scalability of microrobots for industrial production. Researchers are also exploring the use of smart polymers and multifunctional nanoparticles to improve magnetic responsiveness, mechanical strength, and drug-loading capacity. In addition to biomedical applications, magnetic hydrogel microrobots may also be used in environmental monitoring, water purification, targeted chemical delivery, and micro-manufacturing systems. As manufacturing technologies improve and costs decrease, the commercialization of microrobotic systems is expected to increase significantly. Collaboration among biomedical engineers, material scientists, clinicians, and robotics experts will play a major role in transforming laboratory research into practical healthcare solutions. Overall, magnetically actuated hydrogel microrobots represent an advanced therapeutic platform with immense potential to redefine precision medicine, targeted therapy, and future biomedical engineering applications.

CONCLUSION

The present work successfully demonstrated the fabrication and characterization of a PVA–gelatin–Fe₃O₄ based magnetic hydrogel microrobot with promising multifunctional properties for biomedical applications. The combination of synthetic and natural polymers provided a flexible, biocompatible, and mechanically stable hydrogel network, while the incorporation of Fe₃O₄ nanoparticles imparted excellent magnetic responsiveness and heating capability. The freeze–thaw assisted fabrication approach enabled the formation of a stable three-dimensional porous structure with uniform nanoparticle distribution, which is essential for efficient actuation and therapeutic performance. Structural and chemical characterization studies such as FT-IR and XRD confirmed the successful formation of the composite system and verified the presence of characteristic functional groups and crystalline Fe₃O₄ nanoparticles.

Magnetic actuation studies demonstrated that the fabricated microrobot exhibited controlled movement and directional response under external magnetic fields, confirming its suitability for remote navigation in fluidic environments. The observed magnetic responsiveness in PBS medium further validated its stability and functionality under physiologically relevant conditions. In addition, induction heating experiments revealed that the embedded Fe₃O₄ nanoparticles effectively generated localized heat under an alternating magnetic field, achieving temperatures within the therapeutic hyperthermia range. This indicates the potential of the developed system for combined magnetic hyperthermia and targeted therapeutic applications.

Furthermore, the porous hydrogel architecture and soft mechanical nature of the microrobot make it highly suitable for drug loading and controlled release applications. The integration of magnetic guidance, thermal responsiveness, and biocompatibility within a single platform highlights the multifunctional nature of the developed microrobot system. Overall, the study demonstrates that magnetic hydrogel microrobots possess significant potential in advanced biomedical fields such as targeted drug delivery, cancer therapy, minimally invasive treatment, and soft microrobotics. The findings of this work provide a strong foundation for future research focused on improving motion control, drug encapsulation efficiency, and in vivo biomedical performance of magnetic hydrogel microrobotic systems.

CHAPTER 10 REFERENCES

- [1] Mañas-Torres, M. C., Gila-Vilchez, C., Vazquez-Perez, F. J., Kuzhir, P., Momier, D., Scimeca, J. C., ... & Lopez-Lopez, M. T. (2021). Injectable magnetic-responsive short-peptide supramolecular hydrogels: ex vivo and in vivo evaluation. *ACS Applied Materials & Interfaces*, 13(42), 49692-49704.
- [2] Chung, H. J., Parsons, A. M., & Zheng, L. (2021). Magnetically controlled soft robotics utilizing elastomers and gels in actuation: A review. *Advanced Intelligent Systems*, 3(3), 2000186.
- [3] Londhe, P. V., Londhe, M. V., Salunkhe, A. B., Laha, S. S., Mefford, O. T., Thorat, N. D., & Khot, V. M. (2025). Magnetic hydrogel (MagGel): A revolutionary pedestal for anticancer therapy. *Coordination Chemistry Reviews*, 522, 216228.
- [4] Simińska-Stanny, J., Nizioł, M., Szymczyk-Ziółkowska, P., Brożyna, M., Junka, A., Shavandi, A., & Podstawczyk, D. (2022). 4D printing of patterned multimaterial magnetic hydrogel actuators. *Additive Manufacturing*, 49, 102506.
- [5] Wei, X., Wu, Q., Chen, L., Sun, Y., Chen, L., Zhang, C., ... & Jiang, S. (2023). Remotely controlled light/electric/magnetic multiresponsive hydrogel for fast actuations. *ACS Applied Materials & Interfaces*, 15(7), 10030-10043.
- [6] Tang, J., Tong, Z., Xia, Y., Liu, M., Lv, Z., Gao, Y., ... & Wang, T. J. (2018).
- [7] Super tough magnetic hydrogels for remotely triggered shape morphing. *Journal of Materials Chemistry B*, 6(18), 2713-2722
- [8] Kim, D. I., Lee, H., Kwon, S. H., Choi, H., & Park, S. (2019). Magnetic nanoparticles retrievable biodegradable hydrogel microrobot. *Sensors and Actuators B: Chemical*, 289, 65-77.
- [9] Haider, H., Yang, C. H., Zheng, W. J., Yang, J. H., Wang, M. X., Yang, S., ... & Chen, Y. M. (2015). Exceptionally tough and notch-insensitive magnetic hydrogels. *Soft Matter*, 11(42), 8253-8261.
- [10] Chen, Q., Zhang, X., Chen, K., Wu, X., Zong, T., Feng, C., & Zhang, D. (2022). Anisotropic hydrogels with enhanced mechanical and tribological performance by magnetically oriented nanohybrids. *Chemical Engineering Journal*, 430, 133036.
- [11] Kim, D. I., Lee, H., Kwon, S. H., Choi, H., & Park, S. (2019). Magnetic nanoparticles retrievable biodegradable hydrogel microrobot. *Sensors and Actuators B: Chemical*, 289, 65-77.
- [12] Simińska-Stanny, J., Nizioł, M., Szymczyk-Ziółkowska, P., Brożyna, M., Junka, A., Shavandi, A., & Podstawczyk, D. (2022). 4D printing of patterned

multimaterial magnetic hydrogel actuators. *Additive Manufacturing*, 49, 102506.

- [13] Liu, K., Pan, X., Chen, L., Huang, L., Ni, Y., Liu, J., ... & Wang, H. (2018).
- [14] Ultrasoft self-healing nanoparticle-hydrogel composites with conductive and magnetic properties. *ACS Sustainable Chemistry & Engineering*, 6(5), 6395-6403.
- [15] Hu, K., Sun, J., Guo, Z., Wang, P., Chen, Q., Ma, M., & Gu, N. (2015). A
- [16] novel magnetic hydrogel with aligned magnetic colloidal assemblies showing controllable enhancement of magnetothermal effect in the presence of alternating magnetic field. *Advanced Materials*, 27(15), 2507-2514.
- [17] Haider, H., Yang, C. H., Zheng, W. J., Yang, J. H., Wang, M. X., Yang, S., ... & Chen, Y. M. (2015). Exceptionally tough and notch-insensitive magnetic hydrogels. *Soft Matter*, 11(42), 8253-8261.
- [18] Li, S. N., Li, B., Yu, Z. R., Gong, L. X., Xia, Q. Q., Feng, Y., ... & Tang, L.
- [19] C. (2020). Chitosan in-situ grafted magnetite nanoparticles toward mechanically robust and electrically conductive ionic-covalent nanocomposite hydrogels with sensitive strain-responsive resistance. *Composites Science and Technology*, 195, 108173.
- [20] Tang, J., Yin, Q., Qiao, Y., & Wang, T. (2019). Shape morphing of hydrogels in alternating magnetic field. *ACS applied materials & interfaces*, 11(23), 21194-21200.